

## Single-Crystal Growth and Structure Determination of $\text{Ag}_{16}\text{I}_{12}\text{P}_2\text{O}_7$

J. D. GARRETT, J. E. GREEDAN, R. FAGGIANI, S. CARBOTTE,  
AND I. D. BROWN

*Institute for Materials Research, McMaster University, Hamilton,  
Ontario L8S 4M1, Canada*

Received September 25, 1981

Single crystals of the fast-ion conductor  $\text{Ag}_{16}\text{I}_{12}\text{P}_2\text{O}_7$  were prepared and their structure ( $P6/mcc$ ,  $a = 12.054$ ,  $c = 7.504$  Å) was determined by X-ray diffraction ( $r = 0.08$ ). The I atoms form a close-packed array leaving channels occupied by  $\text{P}_2\text{O}_7^{2-}$  ions running along the  $c$  axis. The Ag atoms are disordered over four different types of site with occupation numbers ranging from 0.12 to 0.52. Each  $\text{Ag}^+$  ion coordination polyhedron shares several faces with adjacent polyhedra providing ready paths for  $\text{Ag}^+$  ion conduction.

### Introduction

In an accompanying publication (1), a phase diagram is presented for the system  $\text{AgI}-\text{Ag}_4\text{P}_2\text{O}_7$  and the unusual electrical properties of polycrystalline and single-crystalline  $\text{Ag}_{16}\text{I}_{12}\text{P}_2\text{O}_7$ , a fast-ion electrolyte, are described. Here we describe the growth of single crystals of  $\text{Ag}_{16}\text{I}_{12}\text{P}_2\text{O}_7$  and the solution of the crystal structure, including the location of the silver ions, using automated X-ray diffraction techniques.

### Preparation of Single Crystals

From the phase diagram in (1) the compound  $\text{Ag}_{16}\text{I}_{12}\text{P}_2\text{O}_7$  melts incongruently at  $281^\circ\text{C}$ . However,  $\text{Ag}_{16}\text{I}_{12}\text{P}_2\text{O}_7$  will be the first solid phase to precipitate from any melt within the composition range 14 to 20% molar  $\text{Ag}_4\text{P}_2\text{O}_7$ . A charge containing 15.5%  $\text{Ag}_4\text{P}_2\text{O}_7$  was prepared by coprecipitation from solutions of KI,  $\text{Na}_4\text{P}_2\text{O}_7 \cdot 10\text{H}_2\text{O}$ , and  $\text{AgNO}_3$ . The yellow precipitate was washed with distilled water until free of nitrate ion and vacuum-dried at room temperature. Premelting under a low vacuum ( $10^{-3}$  Torr)

was carried out to consolidate the charge and to eliminate trapped gases. Considerable gas evolution was observed during the premelting step. Upon cooling the quartz ampoule cracked. The premelted charge was a pale yellow glass.

Approximately 17 g of premelted charge was loaded into another quartz ampoule of 8-mm i.d. with a conical tip. The ampoule and contents were sealed under a vacuum of  $10^{-3}$  Torr. A Bridgman geometry was used for the growth experiments. The hot zone temperature was  $280^\circ\text{C}$  and the minimum cold zone temperature was  $150^\circ\text{C}$ . Temperatures were controlled to more than  $\pm 1^\circ\text{C}$  using a Thermac (Research Inc.) three-mode controller. The sample was lowered at about 1 mm/hr, which implied a cooling rate of about  $0.5^\circ\text{K/hr}$  for a duration of 10 days.

The material which had formed in the conical part of the growth crucible showed striations and a distinct cleavage plane. Observation with the polarizing microscope indicated uniaxial symmetry normal to the cleavage plane. Large grains of a few millimeters on a side were recovered which ap-

TABLE I  
 $\text{Ag}_{16}\text{I}_{12}\text{P}_2\text{O}_7$ , HEXAGONAL PARAMETERS

$a = 12.054 (3) \text{ \AA}$	
$c = 7.504 (2) \text{ \AA}$	
$V = 944.2 \text{ \AA}^3$	
$Z = 1$	
Space group: $P6/mcc$	
Conditions for reflection	$hkl: l = 2n$
	$h0l: l = 2n$
Absorption coefficient: $\mu = 17.89 \text{ mm}^{-1}$	
Crystal size: cylinder $r = 0.088 \text{ mm}$	
Density (calcd): $D_x = 6.03$	

parently contained small regions of glassy inclusions as well. However, single crystals of a size suitable for the X-ray diffraction experiments, free of any glassy phase, were obtainable from the bulk grains.

### Structure Determination

The crystals were found from precession photographs to be hexagonal. A crystal was ground to a cylinder of radius 0.09 mm and mounted on a Nicolet P2<sub>1</sub> X-ray diffractometer. The lattice parameters given in Table I

were determined from the positions of 15 well-centered reflections in the range  $20^\circ < 2\theta < 30^\circ$  using monochromatized  $\text{MoK}\alpha$  radiation. The intensities of a total of 1663 reflections were measured at room temperature using a  $\theta/2\theta$  scan and were corrected for Lorentz, polarization, and absorption effects using a cylindrical absorption correction. Two standard reflections measured at intervals during the intensity measurement showed no significant variations. Equivalent reflections were then averaged and systematic absences were removed to give 396 reflections, of which 126 had  $I < 3\sigma(I)$  and were labeled as "unobserved." The positions of the I atoms were readily found since they are the only chemically reasonable positions consistent with the space group. At this stage we became aware of the determination by Geller and Owens (2) of the structure of  $(\text{C}_5\text{H}_5\text{NH})\text{Ag}_5\text{I}_6$ , which has similar lattice parameters, the same space group, and the same arrangement of I atoms. In this compound the pyridinium ions occupy channels

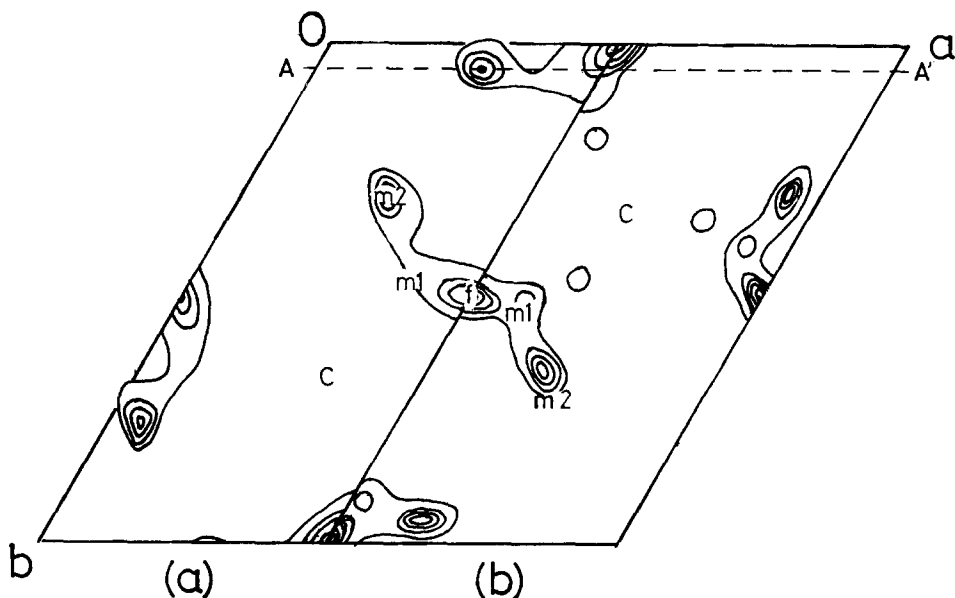


FIG. 1. Positions of Ag atoms in  $\text{Ag}_{16}\text{I}_{12}\text{P}_2\text{O}_7$  (section at  $z = 0.2$ ,  $BB'$  in Fig. 2). (a) X-Ray difference map, (b) atomic probability density predicted from the valence map.

around the sixfold axis and, at low temperatures, the Ag atoms occupy the sites  $6f$  and  $4c$ , the former being surrounded tetrahedrally, and the latter octahedrally, by I atoms. At higher temperatures a four-coordinate  $24m$  site between the  $f$  and  $c$  sites becomes partially occupied, thereby permitting the Ag ions to diffuse through the crystal and contribute to ionic conductivity.

We initially assumed that the  $\text{P}_2\text{O}_7$  ions in  $\text{Ag}_{16}\text{I}_{12}\text{P}_2\text{O}_7$  would replace the pyridinium ions and be disordered on the sixfold axis. We also assumed that at least half the Ag atoms would occupy the  $f$ ,  $c$ , and  $m$  sites. The remaining Ag atoms were expected to lie between the  $\text{P}_2\text{O}_7$  ions and the matrix of I atoms. As this model did not refine, we

prepared an Ag valence "atomic density" map calculated from Waltersson's (3) valence function (see Appendix). This map, Fig. 1b, shows which sites, from a chemical point of view, are best for the Ag atoms. It indicates that the octahedral  $c$  site is not a favorable position. The  $f$  site and its associated  $m$  sites (here called  $m1$  sites) should be occupied, as well as two other sites ( $l$  and  $m2$ ) adjacent to the  $\text{P}_2\text{O}_7$  ions. Placing the 16 Ag atoms on the  $6f$ ,  $24m1$ ,  $24m2$ , and  $12l$  sites resulted in a model that could be refined. Since on the average each site is only one-fourth occupied the occupation number of each Ag atom was also refined. However, these correlate strongly with the temperature factors and it was necessary to

TABLE II  
ATOMIC POSITIONS  $\times 10^4$

Atom	Occupation	x	y	z
Ag( <i>f</i> )	0.52 <sup>a</sup>	5000	0	2500
Ag( <i>m1</i> )	0.12 <sup>a</sup>	947(20)	4747(19)	1605(28)
Ag( <i>m2</i> )	0.29 <sup>a</sup>	2488(7)	9470(8)	1754(16)
Ag( <i>l</i> )	0.26 <sup>a</sup>	489(11)	2467(14)	0
I	1.0	4500(2)	1479(2)	0
P	0.5	0	0	2018(24)
O( <i>b</i> )	0.083	500	200	0
O(1)	0.083	1000	500	3500
O(2)	0.083	-800	-1500	2000
O(3)	0.083	-1000	400	2000

Atom	$U_{11}$ or $U$	TEMPERATURE FACTORS $\times 10^{4b}$				
		$U_{22}$	$U_{33}$	$U_{12}$	$U_{13}$	$U_{23}$
Ag( <i>f</i> )	1700(60)	1700(60)	860(50)	850(30)	0	0
Ag( <i>m1</i> )	1380(160)	1800(210)	920(120)	800(160)	-270(110)	40(120)
Ag( <i>m2</i> )	1070(50)	1050(50)	2320(140)	550(40)	630(70)	650(70)
Ag( <i>l</i> )	740(60)	1420(110)	1330(100)	410(70)	0	0
I	800(10)	620(10)	670(10)	350(10)	0	0
P	430(70)	430(70)	640(190)	210(40)	0	0
O( <i>b</i> )	1340(450)					
O(1)	600					
O(2)	310					
O(3)	660					

<sup>a</sup> The standard errors of 0.004 given by the least-squares refinement for these numbers are too small because of correlations with temperature parameters.

<sup>b</sup> Factors as used in the expression  $\exp(-2\pi^2 \sum_i \sum_j U_{ij} h_i h_j a_i^* a_j^*)$ .

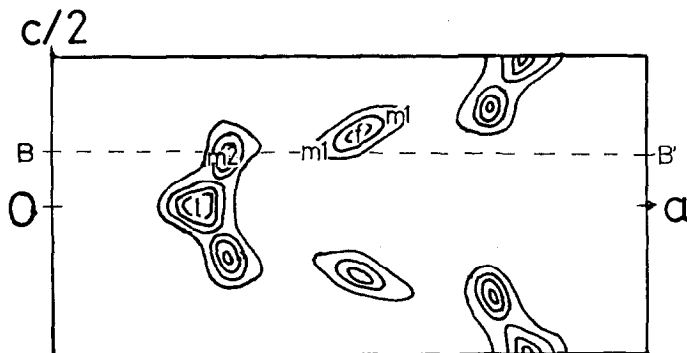


FIG. 2. Positions of Ag atoms in  $\text{Ag}_{16}\text{I}_{12}\text{P}_2\text{O}_7$  (section at  $x = 0.05$ , AA' in Fig. 1). X-Ray difference map.

constrain the occupation numbers to give a total of 16 Ag atoms in the unit cell. Because of this correlation the true standard errors for these parameters will be much larger than the standard errors given in Table II, which are derived from the least-squares refinements and do not take the correlation into account. The space group symmetry requires that the  $\text{P}_2\text{O}_7$  ions possess either  $D_3$ ,  $C_3$ , or  $C_2$  symmetry and be disordered over 12 equivalent positions. On the basis of the observed electron density, a model was chosen in which the P atoms lay on the sixfold axis and the ions had  $C_3$  symmetry. A second  $\text{P}_2\text{O}_7$  ion is then generated by a twofold axis and each of these give rise to a further six ions generated by the sixfold axis. Each of the 12 possible  $\text{P}_2\text{O}_7$  positions would be  $\frac{1}{2}$  occupied.

Even with this disorder, it was possible from a difference synthesis to identify the O atoms. The ion was found to be nonlinear ( $D_3$ ) since the bridging O could be seen lying away from the sixfold axis. It was not possible to refine the O atom coordinates and no significance should therefore be attached to the numerical values of the bond lengths and angles in this group. Isotropic temperature factors were refined for all O atoms except O(1), where the temperature factor tended to become unreasonably large.

In the final refinement the structure fac-

tors were weighted using  $\omega = (\sigma^2 + (kF_0)^2)^{-1}$ , where  $\sigma$  is the standard error from counting statistics and  $k$  was chosen to be 0.03 in order to make  $\langle |\omega(|F_0| - |F_c|)| \rangle$  independent of  $F_0$ . Reflections labeled "unobserved" were assigned  $\omega = 0$  if  $F_0 > F_c$ . The final weighted agreement index,  $(\sum \omega(|F_0| - |F_c|)^2 / \sum \omega |F_0|^2)^{1/2}$ , was 0.084. The standard error in an observation of unit weight was 1.8, but the largest features on the difference map had a height of less than 1.5 electrons  $\text{\AA}^{-3}$  and were all in the neighborhood of heavy atoms. They no doubt reflect the inadequacy of the harmonic approximation to describe the ionic motion in this crystal. Atomic scattering factors were taken from (4).

The final coordinates are given in Table II. Observed and calculated structure factors are given in Table IV<sup>1</sup> and selected

<sup>1</sup> See NAPS document No. 03936 for 3 pages of supplementary material. Order from ASIS/NAPS, Microfiche Publications, P.O. Box 3513, Grand Central Station, New York, N.Y. 10163. Remit in advance \$4.00 for microfiche copy or for photocopy, \$7.75 for up to 20 pages plus \$.30 for each additional page. All orders must be prepaid. Institutions and organizations may order by purchase order. However, there is a billing and handling charge for this service of \$15. Foreign orders add \$4.50 for postage and handling, for the first 20 pages, and \$1.00 for additional 10 pages of material. Remit \$1.50 for postage of any microfiche orders.

TABLE III  
 SELECTED INTERATOMIC DISTANCES

	Occupation number		Anion neighbors	Cation neighbors
$\text{Ag}(f)$	0.52	I	$2.852(2) \times 4$	$\text{Ag}(m1) 1.48(2) \times 4$ $\text{Ag}(m2) 2.82(1) \times 4$
$\text{Ag}(m1)$	0.12	I	2.68(2)	$\text{Ag}(f) 1.48(3)$
		I	2.72(2)	$\text{Ag}(m2) 1.87(2)$
		I	2.87(2)	$\text{Ag}(m1) 2.21(3)$
		I	2.92(3)	$\text{Ag}(m2) 2.39(3)$
				$\text{Ag}(m1) 2.41(3)$
				$\text{Ag}(m1) 2.64(4)$
				$\text{Ag}(m2) 2.69(2)$
				$\text{Ag}(l) 2.79(3)$
$\text{Ag}(m2)$	0.29	O(1)	2.42, 2.65, 2.75, 2.95	$\text{Ag}(l) 1.46(1)$
		O(2)	2.02, 2.15, 2.33, 2.60	$\text{Ag}(m2) 1.57(2)$
		O(3)	1.87, 2.31, 2.47, 2.75	$\text{Ag}(m1) 1.87(2)$
		I	2.76(1)	$\text{Ag}(m2) 2.61(1)$
		I	2.90(1)	$\text{Ag}(m2) 2.63(2)$
		I	2.93(1)	$\text{Ag}(m1) 2.69(2)$
				$\text{Ag}(l) 2.73(1)$
				$\text{Ag}(f) 2.82(1)$
$\text{Ag}(l)$	0.26	O(b)	2.27, 2.31, 2.74, 2.82	$\text{Ag}(m2) 1.46(1) \times 2$
		O(1)	$2.10^a, 2.34^a, 2.95^a$	$\text{Ag}(l) 2.73(1) \times 2$
		O(2)	$2.05^a, 2.34^a, 2.60^a, 2.95^a$	$\text{Ag}(m1) 2.79(3) \times 2$
		O(3)	$1.94^a, 2.68^a, 2.73^a, 2.81^a, 2.92^a$	
		I	2.77(1)	
		I	2.80(2)	

<sup>a</sup> Occurs twice.

interatomic distances in Table III. An electron density difference map showing the positions of Ag in the plane  $z = 0.2$  is given in Fig. 1a, where it is compared with the valence "density" map (Fig. 1b) used to determine the Ag positions. An Ag electron difference map of the plane  $x = 0.05$  is shown in Fig. 2.

### Discussion

The I atoms form a well-defined hexagonal close-packed lattice with large channels, in which lie the disordered  $\text{P}_2\text{O}_7$  ions, running along the  $c$  axis. To this extent the structure is similar to that of  $(\text{C}_5\text{H}_5\text{NH})\text{Ag}_5\text{I}_6$  (2) with  $\text{Ag}_6\text{P}_2\text{O}_7$  replacing

the pyridinium ions. But the arrangement of Ag ions is rather different. In the present compound there are four Ag sites. The  $f$  and  $m1$  site both have four I neighbors, the  $m2$  site has three I and the equivalent of one O neighbor (12 O positions between 1.87 and 3.0 Å, each  $\frac{1}{2}$  occupied), while the  $l$  site has two I and the equivalent of 2.33 O neighbors (28 neighbors between 1.94 and 3.0 Å, each  $\frac{1}{2}$  occupied). Thus each Ag atom has on the average essentially four neighbors. A diagram of the structure showing the I lattice and Ag sites is shown in Fig. 3.

In addition each Ag atom has between six and eight neighboring Ag sites at distances between 1.46 and 2.89 Å. The observed

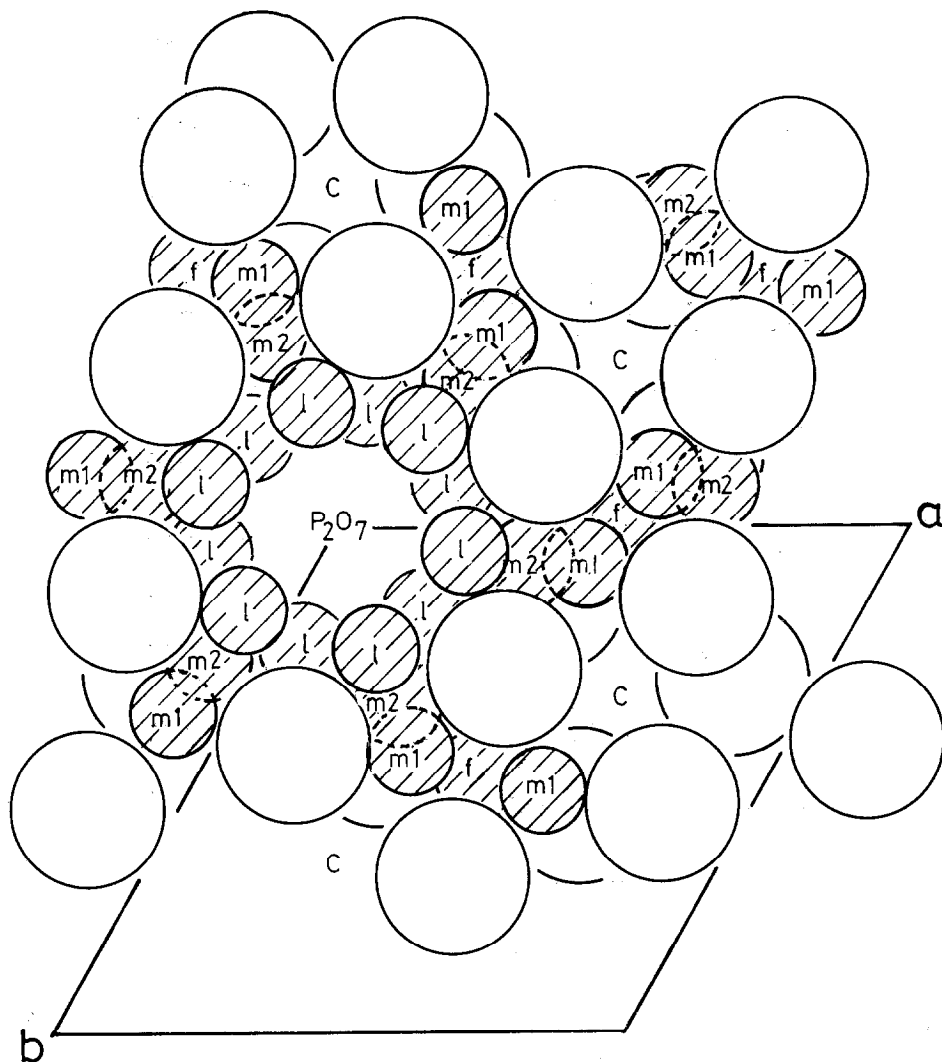


FIG. 3. View of the structure of  $\text{Ag}_{16}\text{I}_{12}\text{P}_2\text{O}_7$  down the  $c$  axis. The large open circles are I at  $z = 0$  and  $\frac{1}{2}$  (mirror planes), the small shaded circles are Ag (shown only over part of the diagram). Atoms of the  $\text{P}_2\text{O}_7$  are not shown. Note the absence of Ag near the  $c$  sites.

occupation numbers for the various sites can be understood if it is assumed that no two sites closer than  $2.7 \text{ \AA}$  can be simultaneously occupied. It is convenient to consider the sites in two groups, an  $f$  site with its four associated  $m1$  sites and an  $l$  site with its two associated  $m2$  sites.

The  $f$  and  $m1$  sites are characterized by each having four I neighbors. Applying the

minimum distance criterion above one finds that it is only possible for one of the five sites in an  $f/m1$  cluster to be occupied. The observed occupation numbers of 0.52 for the  $f$  site and 0.12 for each of the  $m1$  sites add exactly to 1.00, as expected. In the other cluster, in which the Ag atoms are bonded to both I and the  $\text{P}_2\text{O}_7$  ions, the exclusion rule prevents more than a quarter

of the  $m2$  sites being occupied. The observed occupation is 0.29. All  $l$  sites may be filled, the only restriction being that for occupation numbers above 0.75 the occupation of the  $m2$  sites must be correspondingly reduced below 0.25. In fact the occupation number of the  $l$  site is limited by the crystal stoichiometry to 0.33 (assuming the  $m2$  sites are one-quarter filled). The observed occupation number is 0.26. Whether a particular  $l$  or  $m2$  site is occupied will depend on the orientation adopted by the adjacent  $\text{P}_2\text{O}_7$  ions since not all  $l$  sites or all  $m2$  sites will then be equivalent.

An alternative way of looking at the structure is in terms of the packing of cation coordination polyhedra. The disordered O atoms of the  $\text{P}_2\text{O}_7$  ion tend to cluster in groups of six at positions close to 0.10, 0.12, 0.25. Since each O site is  $\frac{1}{2}$  occupied each of these clusters will hold, on the average, half an O atom. Two such groups are needed to give an equivalent coordination number of 1, that is, to be equivalent to one I atom. In the discussion below each of these clusters will be referred to as  $(\text{O}_{1/2})$ . Three types of coordination polyhedra are observed:  $\text{I}_4$ ,  $\text{I}_3(\text{O}_{1/2})_2$ , and  $\text{I}_2(\text{O}_{1/2})_4$ . The  $f$  and  $m1$  sites are both at the center of  $\text{I}_4$  tetrahedra with the  $f$  tetrahedron sharing each of its four faces with a different  $m1$  tetrahedron. The  $m1$  tetrahedron shares one face with the  $f$  tetrahedron, one with an  $m1$  tetrahedron related by the basal mirror plane, and a third face with an  $\text{I}_3(\text{O}_{1/2})_2$  polyhedron containing an  $m2$  site. This site shares faces with two other  $m2$  polyhedra and the  $\text{I}_2(\text{O}_{1/2})_4$  polyhedron around the  $l$  site. Since the  $l$  polyhedron contains a mirror plane it shares two of its faces with  $m2$  polyhedra. Each of the Ag atoms therefore lies in a series of face-connected polyhedra which extend in an infinite network through the crystal. Since each site is only one-fourth occupied on the average, there is plenty of space available for diffusion of the Ag atoms between sites and this diffusion

can occur in any direction in the crystal. It is of interest to note that all of the Ag sites have the major axis of their thermal vibration ellipsoids lying in the plane defined by the neighboring Ag atoms.

## Appendix

### Valence Maps

The principles of inorganic solid-state chemistry have been qualitatively understood for more than half a century (5), but there has been less success in developing quantitative methods for dealing with problems of crystal chemistry. Empirical potential functions have been proposed to deal with specific situations (6), but these usually make the unphysical assumption that the charge on an atom can be treated as a point charge at the nucleus. They also involve fitted parameters that in general are not transferable to other situations.<sup>2</sup>

Although the results of such calculations cannot claim to be rigorous, they generally give a believable estimate of the relative potential in which an atom moves. This appendix examines an alternative empirical approach to the problem.

The concept of bond strength or bond valence originated with Pauling (5). Recently it has been shown (7) that bond valences ( $S$ ) can be determined from the length ( $R$ ) of a bond using a relation such as

$$S = (R/R_0)^{-N},$$

where  $R_0$  and  $N$  are fitted parameters. These parameters are transferable, that is, they need only be determined once for a given pair of atoms and can be used in all crystals where that pair of atoms form a bond. The usefulness of bond valences lies in the empirical rule that the sum of all bond valences received by an atom is equal to its

<sup>2</sup> An obvious exception to this generalization is the recent work on semiempirical two-body potentials for nonbonded contacts in hydrocarbons.

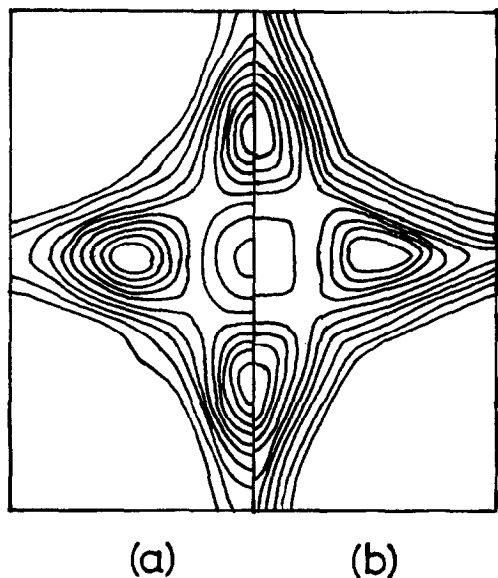


FIG. 4. Ag probability density maps for  $\alpha$ -AgI at  $z = 0$ . (a) Neutron diffraction difference map ( $\delta$ ), (b) predicted from valence map.

atomic valence. This technique can be used to examine the crystochemical plausibility of various proposed models.

Waltersson (3) has used this idea to prepare valence maps. In cases where one type of atom cannot readily be located using standard crystallographic methods (e.g., Li in lithium tungstates), he places the atom in an arbitrary position in the crystal and calculates the valence of the bonds it forms. When the atom is placed at the correct site the sum of its bond valences will be equal to its atomic valence. If the atom is successively placed at a number of different positions in the crystal, a map is produced whose value will be equal to the atomic valence only at chemically acceptable crystal positions for the atom.

Waltersson observed that in many cases a minimum occurs in the valence maps at the correct atomic site. In these cases the form of the valence map is not unlike that of the potential energy. Where there is a low pass between two minima it is not unreasonable

to suppose that this would be an easy diffusion path between two sites since it represents a route along which the empirical valence sum rule could be satisfied with small adjustments of other atomic positions. A similar argument would lead one to expect to see the anisotropy of thermal vibrations reflected in the valence map.

An alternative to calculating a valence map ( $V$ ) is to plot the valence "atomic probability density" ( $D$ ) given by

$$D = V^{-N} \quad (N = \text{constant}).$$

This has maxima at those positions where the valence map had minima and, if  $N$  is chosen to be 16, the resulting  $D$  map bears a remarkable resemblance to the atomic probability density maps determined by diffraction techniques. In particular the valence "density" map for Ag atoms in  $\alpha$ -AgI (Fig. 4) shows the correct positions and shapes of the atoms, as well as the bent diffusion paths between them. Figure 1 gives a similar comparison for  $\text{Ag}_{16}\text{I}_{12}\text{P}_2\text{O}_7$ .

### Acknowledgments

We wish to thank the Natural Science and Engineering Research Council of Canada for operating grants. Collaboration with M. Sayer and his colleagues is gratefully acknowledged.

### References

1. M. SAYER, S. L. SEGEL, J. NOAD, J. COREY, T. BOYLE, R. D. HEYDING, AND A. MANSINGH, *J. Solid State Chem.* **42**, 191 (1982).
2. S. GELLER AND B. G. OWENS, *J. Phys. Chem. Solids* **33**, 1241 (1972).
3. K. WALTERSSON, *Acta Crystallogr. Sect. A* **34**, 901 (1978).
4. "International Tables for X-Ray Crystallography," Vol. IV, p. 72, Kynoch, Birmingham (1974).
5. L. PAULING, *JACS* **49**, 765 (1927).
6. W. H. BAUR, *Acta Crystallogr. Sect. B* **28**, 1456 (1972).
7. I. D. BROWN AND R. D. SHANNON, *Acta Crystallogr. Sect. A* **29**, 266 (1973).
8. R. J. CAVA, F. REIDINGER, AND B. J. WUENSCH, *Solid State Commun.* **24**, 411 (1977).